The effects of Zr and La_2O_3 additions on the microstructural and mechanical properties of a Mo-6Si-5B alloy

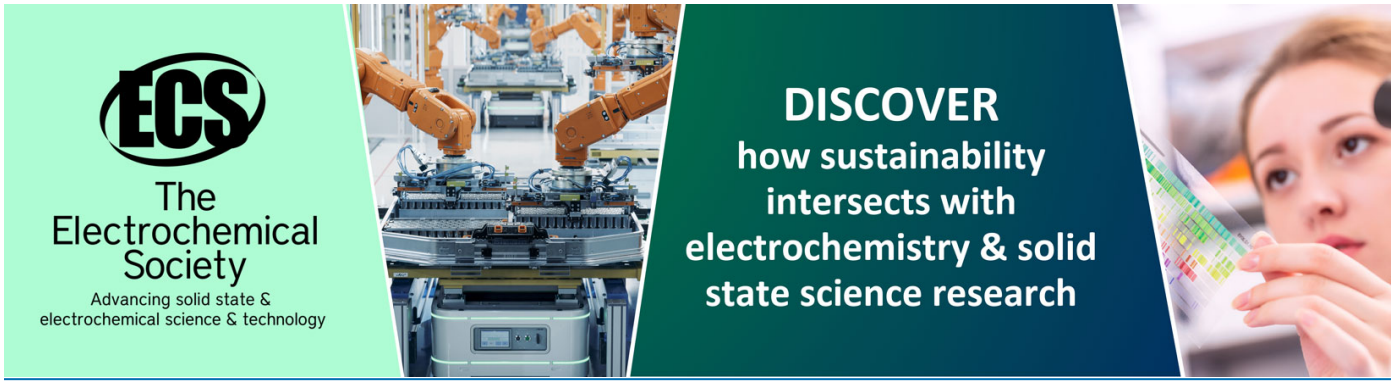

IOP Conf. Series: Materials Science and Engineering **882** (2020) 012001 doi:10.1088/1757-899X/882/1/012001

The effects of Zr and La_2O_3 additions on the microstructural and mechanical properties of a Mo-6Si-5B alloy

J Becker, M Giese and M Krüger

Institute of Materials and Joining Technology, Faculty of Mechanical Engineering, Otto-von-Guericke-University Magdeburg, Universitätsplatz 2, 39106 Magdeburg, Germany

julia.becker@ovgu.de

Abstract. In order to improve the application-related properties, as fracture toughness, creep response and oxidation behavior of Mo-Si-B alloys, certain alloying strategies can be applied. Promising alloying partners like Zr and La_2O_3 may help to enhance the compressive and flexural strength of Mo-Si-B materials. Accordingly, a combination of 1 at.% Zr and 0.5 wt.% La_2O_3 was chosen in order to improve the characteristic properties of a powder metallurgical (PM) Mo-6Si-5B alloy. The influence of Zr and La_2O_3 on the phase distribution and the mechanical properties will be discussed by means of three-point-flexure at room temperature as well as uniaxial compressive creep tests at elevated temperatures (> 1000 °C). Compared with other PM Mo-Si-B alloys the present Zr-La_2O_3-strengthened alloy shows highly improved fracture toughness at room temperature.

1 Introduction

Mo-Si-B alloys have been identified as high-potential materials in numerous comprehensive research studies and are thus promising candidates to replace nickel-based superalloys which are limited in their operating temperatures to a maximum of 1150 °C. Prior investigations show that certain application-related properties, as fracture toughness, creep response and oxidation behavior of those Mo-Si-B alloys [1–3], can be directly affected by their chemical composition according to the ternary phase diagram [4–6] and via different existing manufacturing processes [7–10].

Properties of Mo-Si-B alloys consisting of both brittle as well as ductile phases (silicides and Mo solid solution phase, respectively), are significantly affected by their volume fractions. The thermomechanical stable silicide phases Mo_3Si and Mo_5SiB_2 are mainly responsible for the excellent creep and good oxidation resistance of this group of alloys [2,3,7]. In contrast, the bcc Mo solid solution phase (Mo_{ss}) is responsible for the fracture resistance and brittle-to-ductile transition temperature [1,11–13].

Therefore, the Mo_{ss} phase is a decisive microstructural constituent since it was found to affect the properties of multi-phase Mo-Si-B alloys significantly by its volume fraction, homogeneity and chemical composition [14]. Accordingly, it was reported that Mo-Si-B alloys consisting of a continuously formed Mo_{ss} matrix phase with homogeneously distributed silicides (Mo_3Si and Mo_5SiB_2) show a balanced relation between the application-related properties [7]. With regard to further improvement of the crack and fracture tolerance, recent research focused on avoiding the embrittlement of the Mo_{ss} phase by interstitial as well as solid solution elements. The most critical embrittling element is Si which is dissolved up to concentrations about 3 at.% in technical alloys, reported in [7,13,15].

A promising alloying strategy was developed to improve the ductility and fracture toughness of the Mo_{ss} phase by alloying with Zr, which is mainly due to its getter effect on the detrimental oxygen and the suppressing of Si segregation as well as the formation of ZrO_2 particles and the deflection of cracks

at the phase boundaries [1,11,16,17]. Furthermore, an improvement of hardness and strength was reported due to the formation of nanoscale zirconia particles affecting the microstructure by dispersion strengthening, stabilization of a very fine-grained microstructure as well as increased grain and phase boundary cohesion due to reduced interstitial contamination [18]. Another positive effect was found by alloying with La_2O_3, which predominantly caused grain refinement and particles dispersion strengthening improving both compression and flexure strength of Mo-Si-B alloys [19].

Combining the promising effects of Zr and La_2O_3, this article reports on the impact of alloying additions of 1 at.% Zr and 0.5 wt.% La_2O_3 on the mechanical properties of a Mo-6Si-5B alloy. Microstructural investigations, room temperature three-point-bending tests using notched samples and compressive creep tests at 1093 °C will be applied in order to evaluate the effects on the application-related properties as fracture toughness as well as high temperature creep response. In addition to the reference alloy Mo-6Si-5B, the alloys Mo-9Si-8B and Mo-9Si-8B-1Zr were used to evaluate the creep performance, since these provide similar microstructures and promising creep properties.

2 Materials and Methods

For the present investigations, a Mo-6Si-5B material was alloyed with 1 at.% Zr and 0.5 wt.% La_2O_3, which in the following will be mentioned as the Mo-6Si-5B-1Zr-La_2O_3 alloy. The material was processed by a powder metallurgical (PM) route that included a mechanical alloying (MA) step to achieve fine-grained and chemically homogeneous powder particles. MA was carried out under protective (argon) atmosphere in a planetary ball mill (Retsch PM 400) with a speed of 200 rpm followed by a CIP-sinter-HIP process, detailed described elsewhere [7,20]. For reasons of comparison a similarly processed alloy Mo-6Si-5B was used [7,20].

For microstructure investigations the samples were wet-grinded from 500 down to 1200 grit and the specimen surface was finished by polishing with 3 µm and 1 µm diamond suspension. The microstructural analysis was applied by means of X-ray diffraction measurements using an X'Pert X-ray diffractometer (PANalytical) with Bragg-Brentano geometry and Co - $K_{\alpha 1,2}$ radiation ($\alpha_1 = 1.789$ and $\alpha_2 = 1.793$) and scanning electron microscopy (SEM-FEI ESEM XL30 FEG equipped with EDS, while images were typically obtained in the BSE mode. Quantitative phase analysis was performed using the Rietveld method with the Topas Academic V5 program package (A.A. Coelho, Topas Academic V5, Coelho Software) and the crystal structures of Mo, Mo_3Si, and Mo_5SiB_2 as starting parameters, detailed described elsewhere [21].

The room-temperature fracture strength was applied performing three-point-bending tests on notched bending specimen with dimensions of 2 mm x 2 mm x 18 mm (DIN EN ISO 23146). In a first step, the ground and polished bending specimen were provided with a pre-notch using electrical discharge machining (EDM), ending up with a notch geometry of 0.8 mm in depth and less than 0.2 mm in width. A "sharp crack" with typical depth of 200 µm and a tip radius of around 10 µm was produced using a self-built cutting device equipped with a razor blade working with 1 µm diamond paste. In order to control the notch depth and tip-radius, the samples were examined at defined intervals (15 – 20 min) using an optical microscope.

Fracture toughness measurements were then performed applying a minimum number of five samples having similar notch base radii of around 10 µm. Three-point flexure was realized using a microtest cell (Materials Testing Nano Tomography Version 3.2, Deben) at ambient temperature with a load rate of 0.5 mm/min after preloading with 2 N. The determination of fracture toughness was carried out as described elsewhere [21]. The compressive creep behavior was determined on EDM-cut samples with dimensions of 2 mm x 2 mm x 3.5 mm, tested under constant true stress using a Zwick electromechanical testing device equipped with a Maytec furnace at a temperature of 1093 °C. This temperature was chosen to ensure the comparability to other Mo-Si-B alloys tested at 2000 °F (= 1093 °C).

3 Results and Discussion

3.1 Microstructural investigations

Representative micrographs of the PM alloys are shown in Figure 1. In case of the Zr-La_2O_3-added alloy, a finer-grained microstructure can be observed with an average grain size of 0.7 µm, which represents a reduction of 56 % compared with alloy Mo-6Si-5B [7] having an average grain size of 1.6 µm.

According to X-ray diffraction (Figure 1c and [7]), both alloys exhibit the typical three-phase microstructure of Mo_{ss}-Mo_3Si-Mo_5SiB_2. However, the additions of 1 at.% Zr and 0.5 wt.% La_2O_3 are of a very low quantity in order to detect them via XRD measurements.

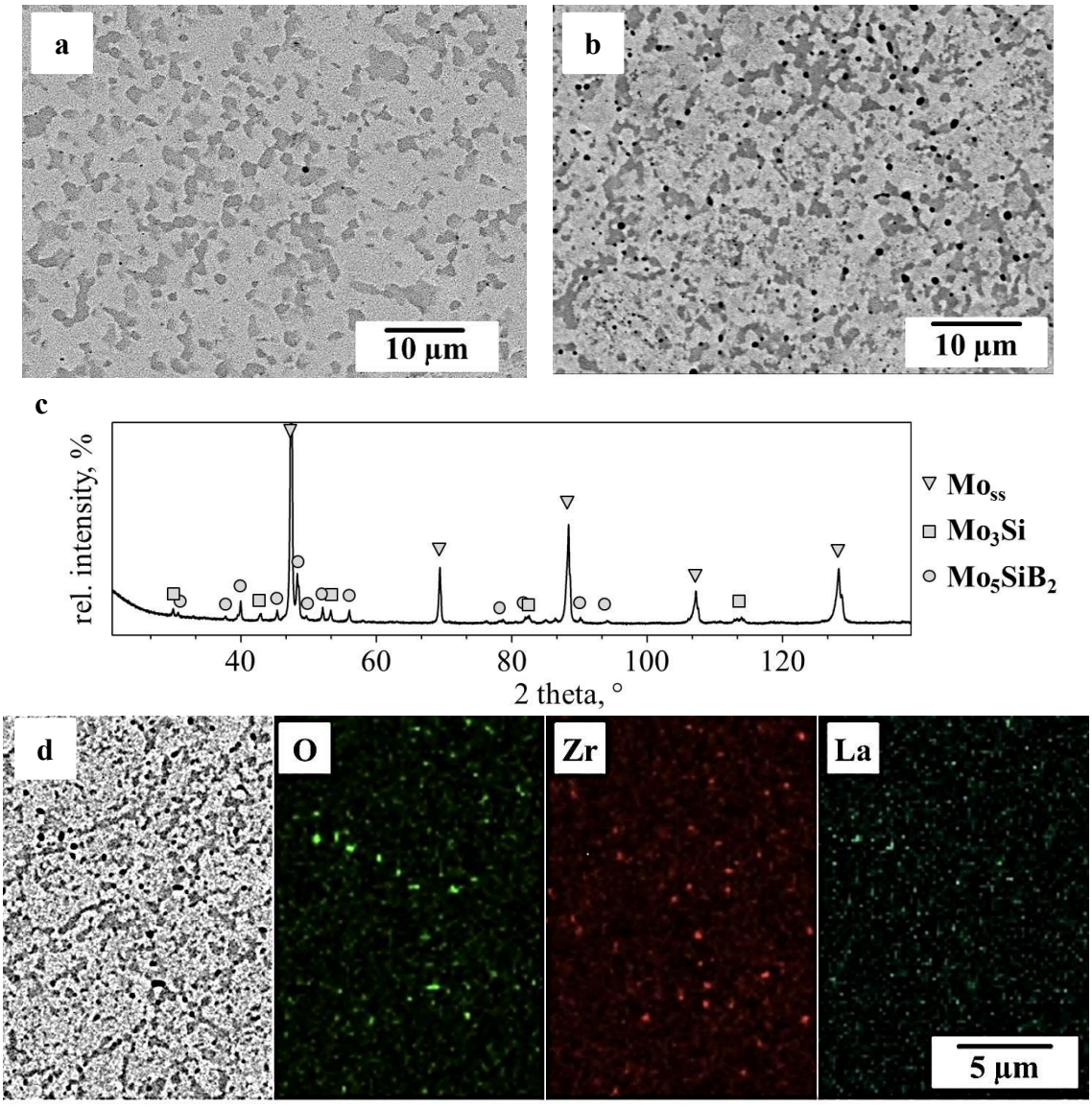

Figure 1. BSE micrograph of alloy (a) Mo-6Si-5B, (b) Mo-6Si-5B-1Zr-La_2O_3 (c) X-ray diffraction patterns of Mo-6Si-5B-1Zr-La_2O_3 showing the existence of three phases: Mo_{ss}, Mo_3Si and Mo_5SiB_2 and (d) EDS element mapping for O, Zr and La_2O_3 in Mo-6Si-5B-1Zr-La_2O_3.

Apart from that, EDS element mapping for the elements O, Zr and La, depicted in Figure 1d, illustrate that the black particles within the microstructure of Mo-6Si-5B-1Zr-La_2O_3 are mainly ZrO_2. However, also a small amount of SiO_2 particles might be present since not every individual oxygen-containing

particle could be identified either as Zr or La oxide. So, this illustrates the oxygen gettering effect by Zr, since in Mo-6Si-5B all the black particles are SiO_2. Due to the mechanical alloying process, most of the La_2O_3 particles are very small and therefore, difficult to be detected by EDS. From the EDS mapping in Figure 1d it can be assumed that La_2O_3 particles are finely dispersed within the microstructure. Both materials, the reference alloy and the Zr-La_2O_3-modified alloy exhibit continuously formed Mo_{ss} matrices with finely distributed intermetallic phases Mo_3Si and Mo_5SiB_2. With 74 vol.% Mo_{ss} and 26 vol.% intermetallic phases (IP) in Mo-6Si-5B-1Zr-La_2O_3, the amounts of the corresponding phases are similar to the Mo-6Si-5B alloy (70 vol.% Mo_{ss} : 30 vol.% IP).

3.2 Impact of Zr- and La_2O_3- alloying on the room temperature fracture toughness

Figure 2a shows a comparison of the fracture toughness of different Mo-Si-B alloys arranged by their increasing amount of continuous or discontinuous Mo_{ss} phase. The room temperature fracture toughness of the intermetallic phases with 1.5...3 $MPam^{1/2}$ [22] is significantly lower than for pure Mo (24 $MPam^{1/2}$ [15]). Therefore, fracture toughness values of Mo-Si-B alloys as reported in literature are typically in between 6 and 16 $MPam^{1/2}$.

In general, depending on the chemical composition (Si and B concentration) and the manufacturing process a continuous Mo_{ss} or silicide matrix (discontinuous Mo_{ss}) forms. As illustrated in Figure 2a, the fracture toughness of Mo-Si-B alloys can be divided into two groups: The alloys having a silicide matrix (black symbols - discontinuous Mo_{ss}) exhibit typical fracture toughness values between 6 and 7.4 $MPam^{1/2}$ and alloys having a continuous Mo_{ss} matrix (open symbols) provide values between 11 and 18.8 $MPam^{1/2}$. The Mo-6Si-5B-1Zr-La_2O_3 alloy has a nearly continuous Mo_{ss} matrix phase and the fracture toughness of 18.8 $MPam^{1/2}$ exceeds the values for this type of alloys given in the literature. This is assumed due to the following reasons: (I) the high amount of Mo_{ss} phase, (II) and its continuous distribution, (III) the very fine microstructure of Mo_{ss} phase after alloying with Zr and La_2O_3, which according to Schneibel et al. [23] also affects the fracture toughness and (IV) reduced embrittlement of grain boundaries by gettering the detrimental oxygen accompanied with the formation of ZrO_2 [17].

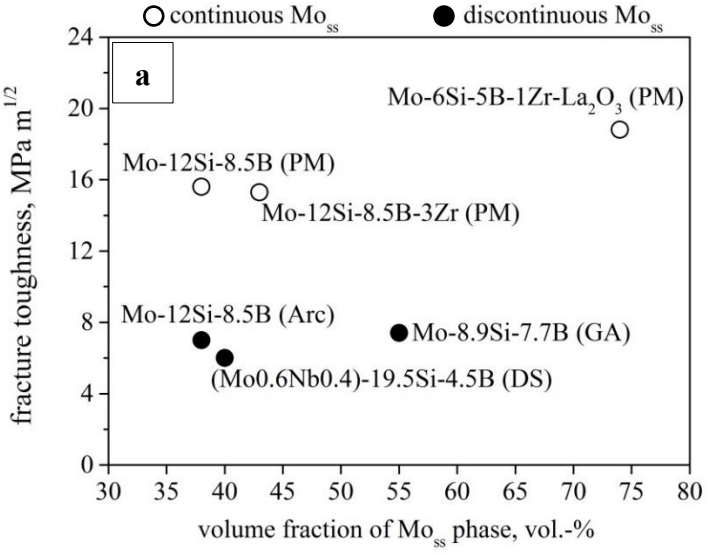

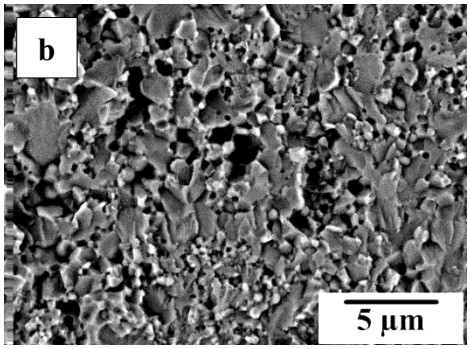

Figure 2. Comparison of fracture toughness values for Mo-6Si-5B-1Zr-La_2O_3 with other Mo-Si-B alloys [1,23–26] (a) and (b) fracture surface of Mo-6Si-5B-1Zr-La_2O_3 after three-point bending.

As depicted in Figure 2b alloy Mo-6Si-5B-1Zr-La_2O_3 shows a mixed fracture mode of predominantly transgranular fracture in Mo_{ss} but also intergranular fracture, the latter within the silicide phases. Metallographic observations of cracked samples show interactions between the Mo_{ss} phase and the intermetallic phases, i.e. crack deflection and crack interception which were also identified in other fine-grained Mo-Si-B materials with homogeneous microstructures, e.g. in [1]. These effects are due to a high probability of the interaction of the crack path with the ductile Mo_{ss} phases.

3.3 Effects of Zr and La_2O_3 on the creep properties of Mo-6Si-5B

The high temperature creep performance of the Mo-6Si-5B-1Zr-La_2O_3 alloy at 1093 °C was comparatively investigated with other PM processed alloys, consisting of a Mo_{ss}-Mo_3Si-Mo_5SiB_2 three-phase microstructure and continuous Mo_{ss} matrix phase. The corresponding Norton-plot is illustrated in Figure 3 at a temperature of 1093 °C, as a typical service temperature in high pressure turbines. For reasons of comparison previously analyzed creep data are included.

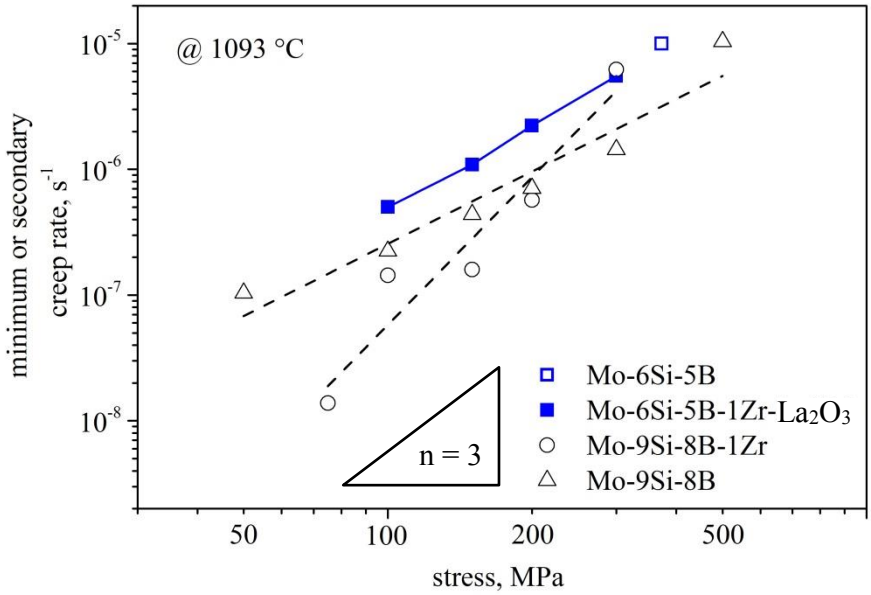

Figure 3. Double-logarithmic plot of the creep rate vs. constant stress at 1093°C for Mo-6Si-5B-1Zr-La_2O_3 compared with other Mo-Si-B alloys.

For the reference alloy Mo-6Si-5B there is only one data point available, which at least allows the assumption, that the creep performance in case of Mo-6Si-5B-1Zr-La_2O_3 may be slightly improved by the effects of alloying additions Zr and La_2O_3. In case of alloy Mo-6Si-6B-1Zr-La_2O_3 this might be explained by the mutual impact of strengthening particles which are thermally stable and reduce the creep deformation by providing obstacles to dislocation movement at high temperatures. On the other hand, the Mo-6Si-5B benefits from the larger grain size providing less creep deformation in case of grain boundary sliding.

Compared to the reference alloy Mo-9Si-8B (HIP) the Mo-6Si-5B-1Zr-La_2O_3 alloy is slightly weaker under similar creep loading. Assuming power law creep, the stress exponent is expressed as the slope $n = \Delta \log \dot{\varepsilon} / \Delta \log \sigma$ of straight lines in Figure 3. The stress exponent for Mo-6Si-5B-1Zr-La_2O_3 was found to be 2.2 and 1.9 for Mo-9Si-8B, which indicates grain boundary sliding and dislocation climb-controlled creep, which can be rationalized by the fine-grained microstructure of this type of PM alloys. Accordingly, the creep resistance may be improved by a grain growth heat treatment [27]. In comparison, the alloy Mo-9Si-8B-1Zr, which yields a stress exponent of 3.9, shows a faster weakening especially above 150 MPa. The reasons of more significant weakening of Mo-9Si-8B and Mo-9Si-8B-1Zr at higher stresses are not clarified, yet.

At temperatures lower than 1100 °C crept Mo-Si-B samples typically show dislocation activities only in the Mo_{ss} phase, which has the lowest creep resistance in this multi-phase system [28]. Since the amount of Mo_{ss} is comparably higher (74 vol.%) than in Mo-9Si-8B (~ 50 vol.%) and Mo-9Si-8B-1Zr the creep response is mainly driven by the plastic deformation of the Mo_{ss} matrix. Considering those conditions, the creep response of the Zr-La_2O_3-modified alloy is comprehensible.

4 Summary and Conclusions

The present investigations showed how small additions of Zr and La_2O_3 can affect the room and high temperature properties of PM Mo-Si-B alloys. Finally, the following conclusions can be drawn:

1. The addition of 1 at.% Zr and 0.5 wt..% La_2O_3 to a Mo-6Si-5B alloy leads to a grain refinement of about 56 %. Instead of SiO_2 particles, ZrO_2 formed, due to the getter effect on the detrimental oxygen. The La_2O_3 particles are finely dispersed within the microstructure.
2. The fracture toughness could be highly improved up to 18.8 $MPam^{1/2}$ due to the high amount (74 vol.%) of Mo_{ss} matrix phase, but also caused by the grain refinement as well as grain boundary strengthening due to ZrO_2 and La_2O_3 particles.
3. The creep response of Mo-6Si-5B-1Zr-La_2O_3 can be well explained in comparison with other PM Mo-Si-B alloys. The Zr- and La_2O_3-modified alloy shows comparable creep exponents, indicating grain boundary sliding and dislocation climb-controlled creep. Since the amount of Mo_{ss} is higher than in other PM Mo-Si-B alloys used for comparison, the creep response is mainly driven by the plastic deformation of the Mo_{ss} matrix.

Acknowledgements

We acknowledge for funding by the DFG graduate school 1554 “Micro-macro interactions in structured media and particle systems” (funding number: 83477795).

References

[1] Li R, Li B, Wang T, Ren S, Chen X, Wang J and Zhang G 2018 Improved fracture toughness of a Mo-12Si-8 . 5B-3Zr alloy by grain coarsening and its multiple toughening mechanisms *J. Alloys Compd.* **743** 716–27

[2] Azim M A, Schliephake D, Hochmuth C, Gorr B, Christ H J, Glatzel U and Heilmaier M 2015 Creep Resistance and Oxidation Behavior of Novel Mo-Si-B-Ti Alloys *JOM* **67** 2621–8

[3] Rioult F A, Imhoff S D, Sakidja R and Perepezko J H 2009 Transient oxidation of Mo-Si-B alloys: Effect of the microstructure size scale *Acta Mater.* **57** 4600–13

[4] Nowotny E, Dimakopoulou and Kudielka H 1957 Untersuchungen in den Dreistoffsystemen : Molybdän-Silizium-Bor, Wolfram-Silizium-Bor und in dem System : VSi2-TaSi2 *Monatshefte für Chemie und verwandte Teile anderer Wissenschaften* **88** 180–92

[5] Hasemann G, Ida S, Zhu L, Iizawa T, Yoshimi K and Krüger M 2020 Experimental assessment of the microstructure evolution and liquidus projection in the Mo-rich Mo–Si–B system *Mater. Des.* **185** 108233

[6] Soboyejo W O and Srivatsan T S 2006 *Advanced Structural Materials: Properties, Design Optimization, and Applications* (Boca Raton: CRC Press)

[7] Krüger M, Jain P, Kumar K S and Heilmaier M 2014 Correlation between microstructure and properties of fine grained Mo-Mo_3Si-Mo_5SiB_2 alloys *Intermetallics* **48** 10–8

[8] Krüger M, Hasemann G, Bogomol I and Loboda P I 2012 Multiphase Mo-Si-B alloys processed by diractional soldification.pdf 303–8

[9] Ihara K, Ito K, Tanaka K and Yamaguchi M 2002 Mechanical properties of Mo 5 SiB 2 single crystals *Mater. Sci. Eng. A* **329**–**331** 222–7

[10] Schmelzer J, Rittinghaus S-K, Weisheit A, Stobik M, Paulus J, Gruber K, Wessel E, Heinze C and Krüger M 2019 Printability of gas atomized Mo-Si-B powders by laser metal deposition *Int. J. Refract. Met. Hard Mater.* **78** 123–6

[11] Saage H, Krüger M, Sturm D, Heilmaier M, Schneibel J H, George E, Heatherly L, Somsen C, Eggeler G and Yang Y 2009 Ductilization of Mo-Si solid solutions manufactured by powder metallurgy *Acta Mater.* **57** 3895–901

[12] Moriyama T, Yoshimi K, Zhao M, Masnou T, Yokoyama T, Nakamura J, Katsui H and Goto T 2017 Room-temperature fracture toughness of MoSiBTiC alloys *Intermetallics* **84** 92–102

[13] Jain P and Kumar K S 2010 Dissolved Si in Mo and its effects on the properties of Mo-Si-B alloys *Scr. Mater.* **62** 1–4

[14] Becker J and Krüger M 2015 Impact of Phase Distribution on the Fracture Toughness of High Temperature Resistant Mo-Si-B Alloys Der Einfluss der Phasenverteilung auf die Bruchzähigkeit von hochtemperatur- beständigen Mo-Si-B-Legierungen *Pract. Metallogr.* **52** 295–313
[15] Sturm D, Heilmaier M, Schneibel J H, Jéhanno P, Skrotzki B and Saage H 2007 The influence of silicon on the strength and fracture toughness of molybdenum *Mater. Sci. Eng. A* **463** 107–14
[16] Geller C B, Smith R W, Hack J E, Saxe P and Wimmer E 2005 A computational search for ductilizing additives to Mo *Scr. Mater.* **52** 205–10
[17] Krüger M, Kauss O, Naumenko K, Burmeister C, Wessel E and Schmelzer J 2019 Intermetallics The potential of mechanical alloying to improve the strength and ductility of Mo – 9Si – 8B – 1Zr alloys – experiments and simulation *Intermetallics* **113** 106558
[18] Krüger M, Schliephake D, Jain P and Kumar K S 2013 Effects of Zr Additions on the Microstructure and the Mechanical Behavior of PM Mo-Si-B Alloys *JOM* **65** 301–6
[19] Zhang G, Zha Y, Li B, He W and Sun J 2013 Effects of lanthanum oxide content on mechanical properties of mechanical alloying Mo – 12Si – 8 . 5B (at .%) alloys *Int . J. Refract. Met. Hard Mater.* **41** 585–9
[20] Krüger M, Franz S, Saage H, Heilmaier M, Schneibel J H, Jéhanno P, Böning M and Kestler H 2008 Mechanically alloyed Mo-Si-B alloys with a continuous $α$-Mo matrix and improved mechanical properties *Intermetallics* **16** 933–41
[21] Becker J, Betke U, Hoffmeister M and Krüger M 2018 Density Reduction of Mo-Si-B Alloys by Vanadium Alloying *JOM* **70** 2574–2581
[22] Mitra R 2006 Mechanical behaviour and oxidation resistance of structural silicides *Int. Mater. Rev.* **51** 13–64
[23] Schneibel J H, Kramer M J and Easton D S 2002 A Mo-Si-B intermetallic alloy with a continuous α-Mo matrix *Scr. Mater.* **46** 217–21
[24] Jéhanno P, Heilmaier M and Kestler H 2004 Characterization of an industrially processed Mo-based silicide alloy *Intermetallics* **12** 1005–9
[25] Choe H, Chen D, Schneibel J H and Ritchie R O 2001 Ambient to high temperature fracture toughness and fatigue-crack propagation behavior in a Mo - 12Si - 8.5B (at.%) intermetallic *Intermetallics* **9** 319–29
[26] Ito K, Kumagai M, Hayashi T and Yamaguchi M 2003 Room temperature fracture toughness and high temperature strength of T2/Moss and (Mo, Nb)ss/T1/T2 eutectic alloys in the Mo-Si-B system *Scr. Mater.* **49** 285–90
[27] Jéhanno P, Heilmaier M, Saage H, Böning M, Kestler H, Freudenberger J and Drawin S 2007 Assessment of the high temperature deformation behavior of molybdenum silicide alloys *Mater. Sci. Eng. A* **463** 216–23
[28] Jain P and Kumar K S 2010 Tensile creep of Mo – Si – B alloys *Acta Mater.* **58** 2124–42